**TITLE**: Pharmacokinetic evaluation of new drugs using a multi-labelling approach and PET imaging: application to a drug candidate with potential application in neuromuscular disorders.

**Authors' full names:** Rossana Passannante,[1] Vanessa Gómez-Vallejo,[1] Maialen Sagartzazu-Aizpurua,[2] Laura Vignau,[2] Pablo Marco-Moreno,[3,4] Garazi Aldanondo,[4] Ainara Vallejo-Illarramendi,[3,4] Pablo Aguiar,[5] Unai Cossío,[1] Abraham Martín,[6,7] Jonas Bergare,[8] Lee Kingston,[8] Charles S. Elmore,[8] Miguel Angel Morcillo,[9] Pablo Ferrón,[10] Jesus M. Aizpurua,[2] Jordi Llop,[1,*]

**Authors' affiliation(s):**

[1] CIC biomaGUNE, Basque Research and Technology Alliance (BRTA), 20014-San Sebastián, Spain

[2] Departamento de Química Orgánica-I, UPV/EHU-University of the Basque Country, 20018-San Sebastián, Spain

[3] Group of Neuroscience, Department of Pediatrics, Hospital Donostia, UPV/EHU, 20014-San Sebastián, Spain

[4] Group of Neuromuscular Diseases. Biodonostia Health Research Institute, 20014-San Sebastián, Spain

[5] Molecular Imaging Group, IDIS, CIMUS, Universidad de Santiago de Compostela, Spain

[6] Ikerbasque, Basque Foundation for Science, Maria Diaz de Haro 3, 48013-Bilbao, Spain.

[7] Laboratory of Neuroimaging and biomarkers of inflammation, Achucarro Basque Center for Neuroscience, Science Park UPV/EHU, Sede building B, Sarriena, 48940-Leioa, Spain

[8] Early Chemical Development, Pharmaceutical Sciences R&D, AstraZeneca, 431 83-Gothenburg, Sweden

[9] CIEMAT, Medical Applications of Ionizing Radiations Unit, Madrid, Spain

[10] Miramoon Pharma S.L., Avda Tolosa-72, 20018-San Sebastián, Spain

**Corresponding author details:**

Name: Jordi Llop

Email: jllop@cicbiomagune.es

**Figure S1.** a) Reaction scheme for the production of [$^{11}$C]AHK2.1; b) Chromatograph (radioactivity detector) obtained after analysis of the reaction crude in the production of [$^{11}$C]AHK2.1; c) Chromatograph (radioactivity detector) obtained during purification of the reaction crude in the production of [$^{11}$C]AHK2.1. The peak corresponding to [$^{11}$C]AHK2.1 (green area) was collected and reformulated.

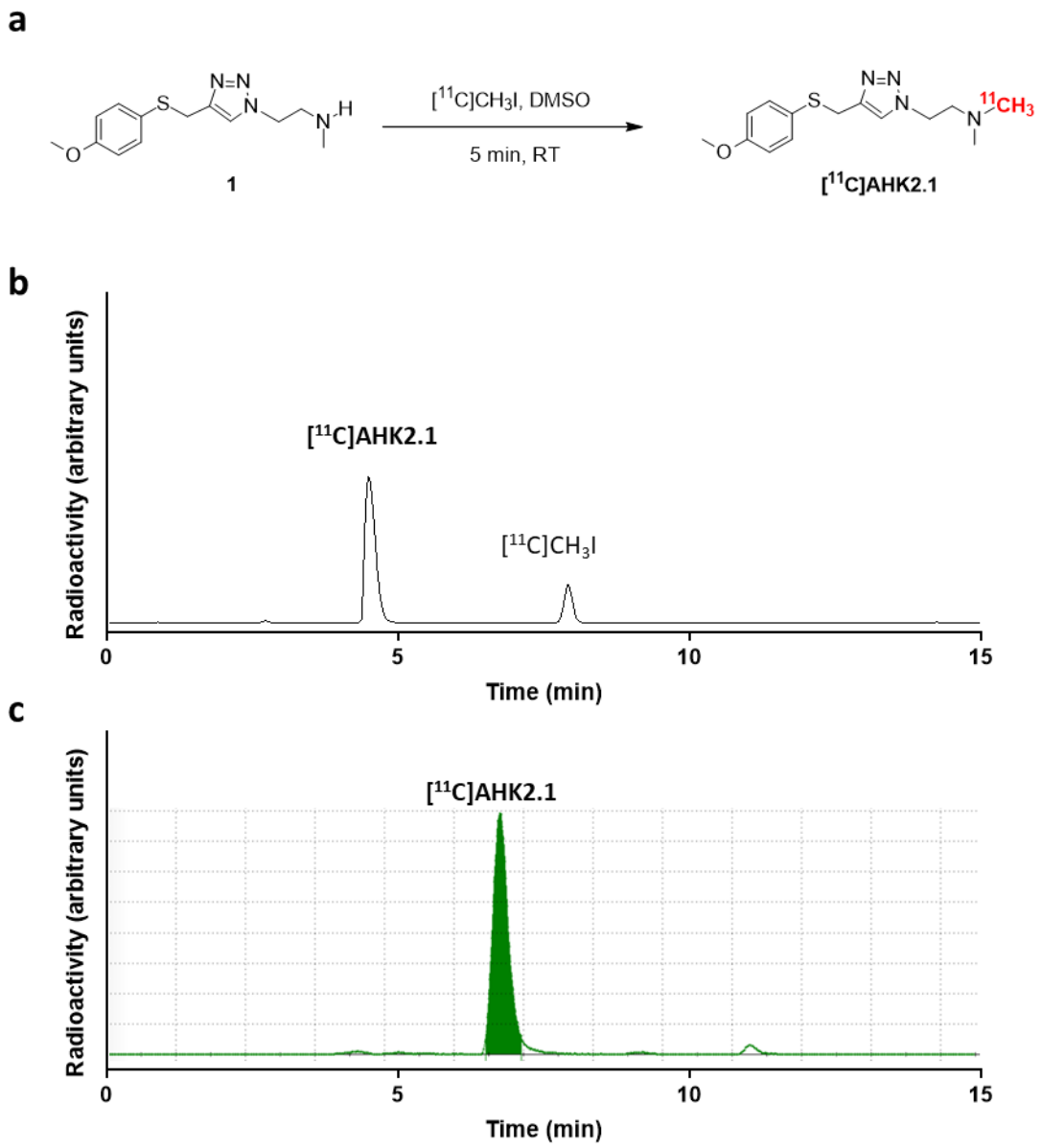


**Figure S2.** a) Reaction scheme for the production of [$^{11}$C]AHK2.2; b) Chromatographs (radioactivity detector) obtained after analysis of the reaction crude in the production of [$^{11}$C]AHK2.2 using NaOH (top) and NaH (bottom) as the base; c) Chromatograph (radioactivity detector) obtained during purification of the reaction crude in the production of [$^{11}$C]AHK2.2. The peak corresponding to [$^{11}$C]AHK2.2 (green area) was collected and reformulated.

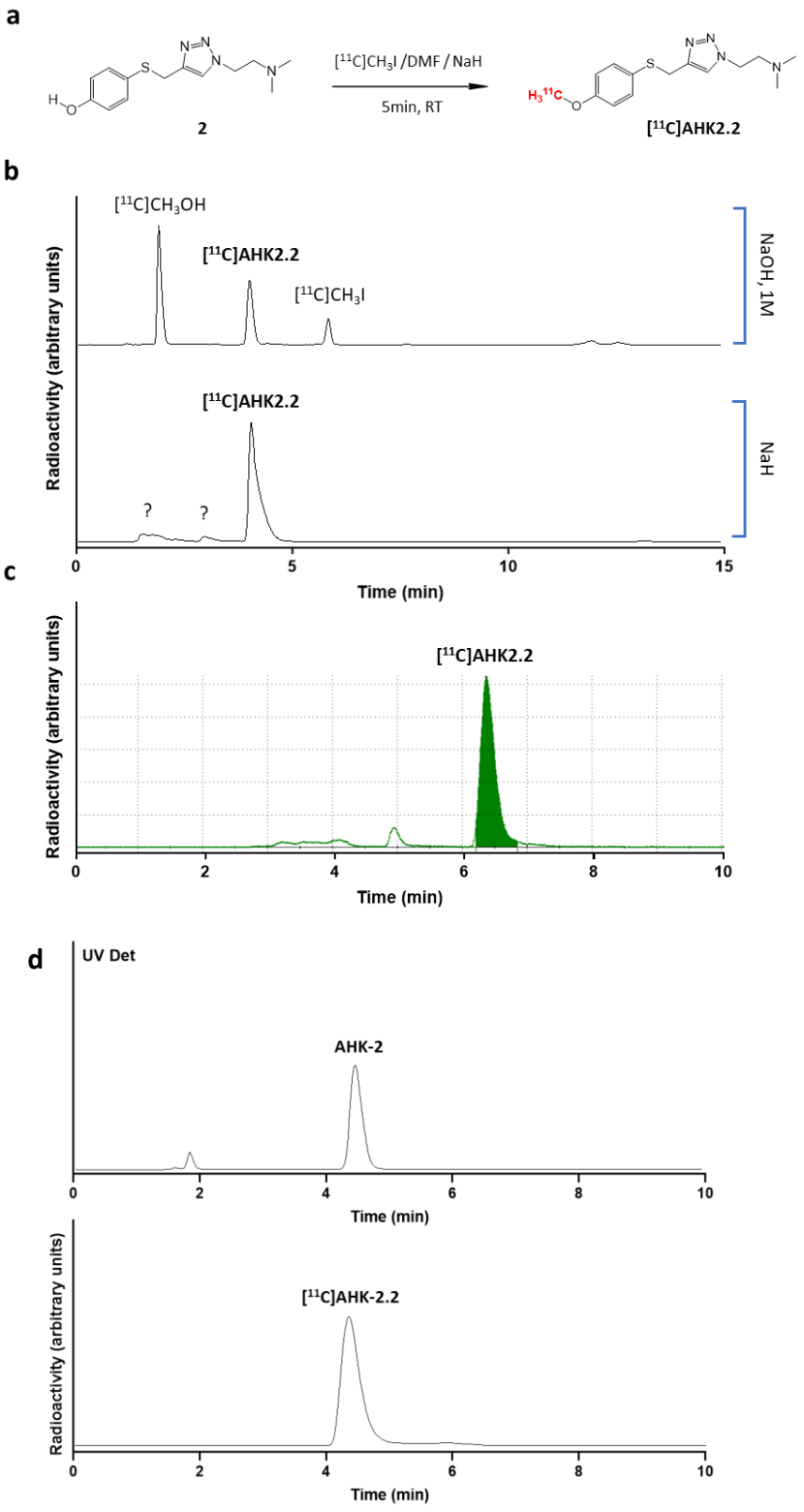


**Figure S3.** a) Reaction scheme for the production of [$^3$H]AHK2; b,c) Chromatographs (UV and radioactivity detectors, respectively) obtained after purification of [$^3$H]AHK2; d) mass spectrum of the indicated chromatographic peak, confirming the formation of [$^3$H]AHK2.

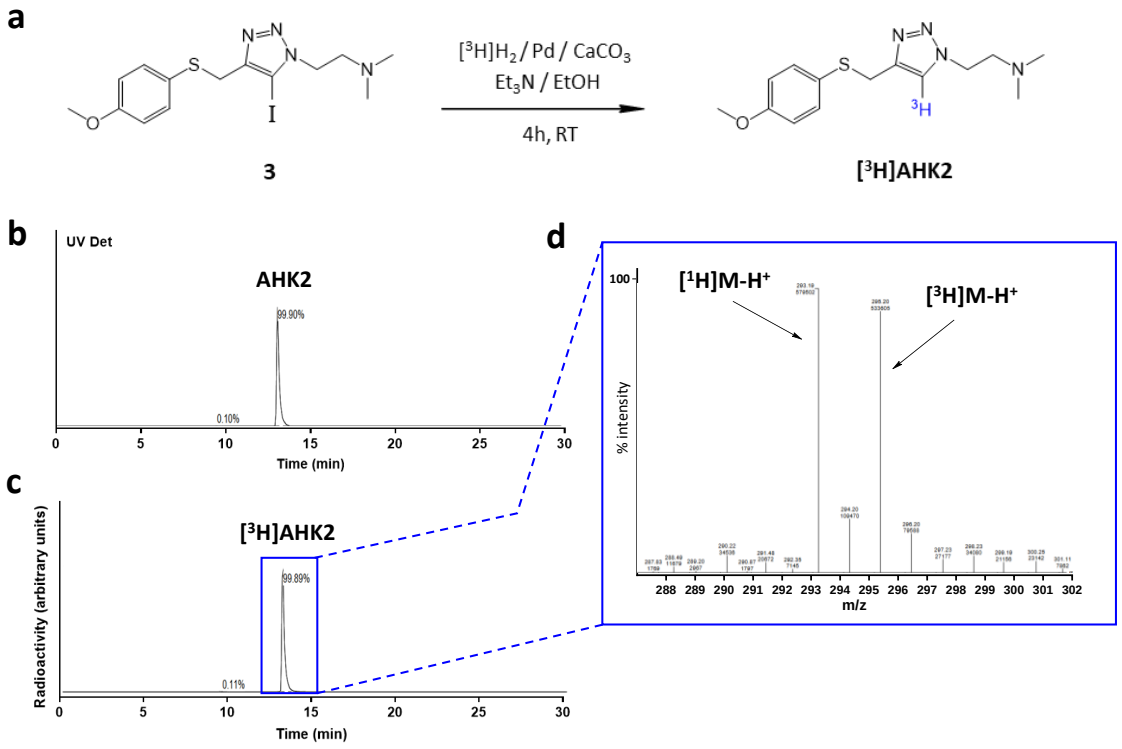


**Figure S4.** Representative chromatograms (radioactivity detector) corresponding to the evaluation of the presence of metabolites in plasma after intravenous administration of [$^{11}$C]AHK2.1 (a) and [$^{11}$C]AHK2.2 (b) at injected dose = 1 µg/Kg. The position of the peaks corresponding to major metabolites are shown.

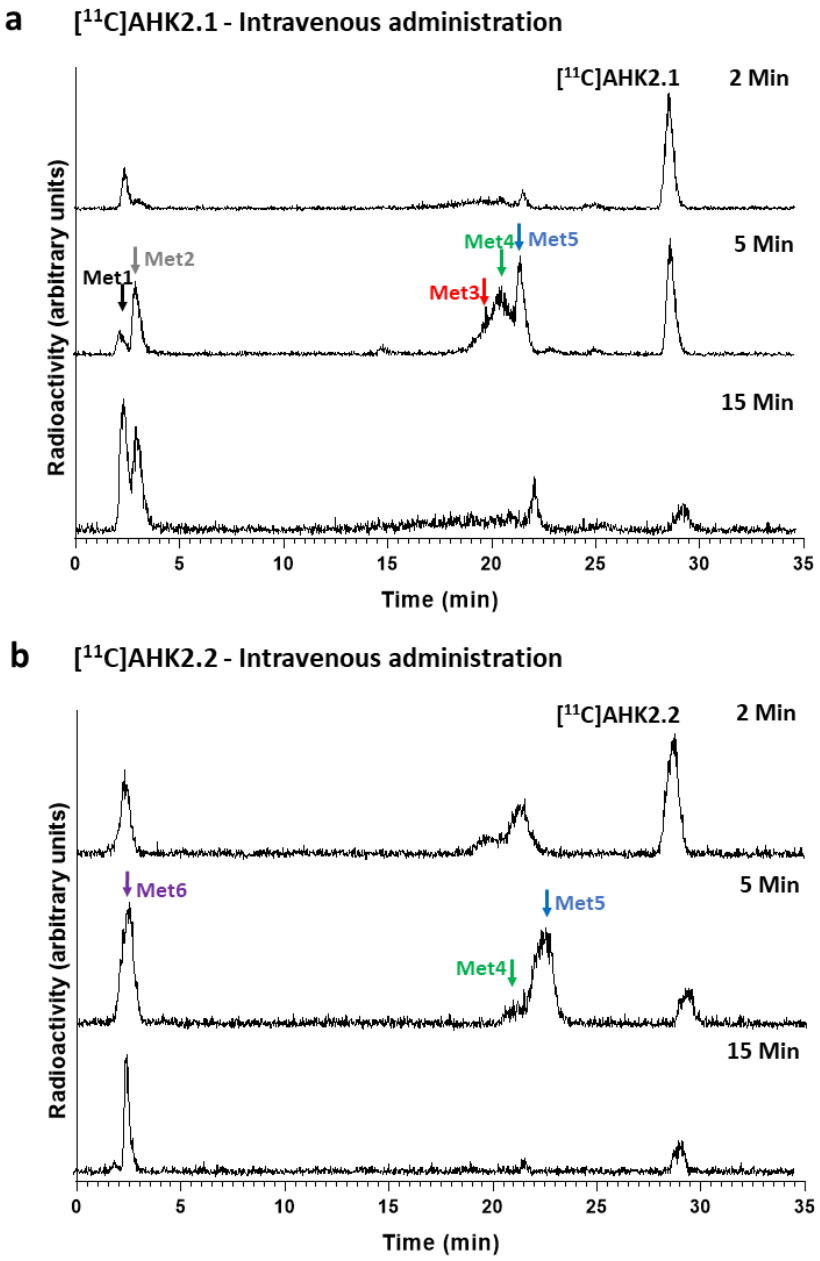


**Figure S5.** Representative chromatograms (radioactivity detector) corresponding to the evaluation of the presence of metabolites in plasma after oral administration of [$^{11}$C]AHK2.1 (a) and [$^{11}$C]AHK2.2 (b) at injected dose = 1 µg/Kg. The position of the peaks corresponding to major metabolites are shown.

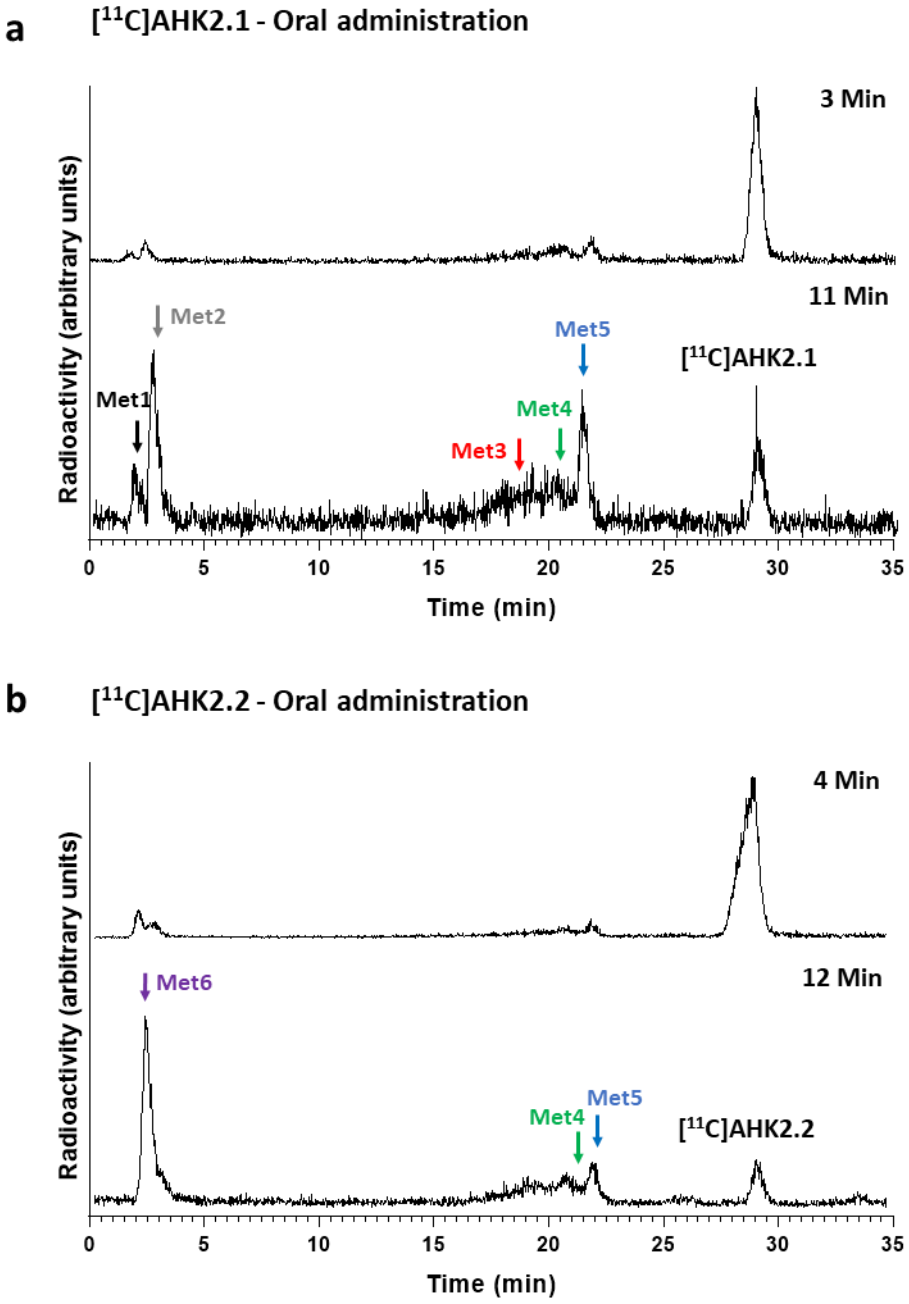


**Figure S6.** a) Representative arterial plasma Time Activity Curves (TACs) after oral administration of [$^{11}$C]AHK2.1 at [1 µg/Kg] (left) and [5 mg/Kg] (right); b) graphic representation of plasma concentration over time of AHK2 after intravenous administration of $^{11}$C-labelled AHK2 at [1 µg/Kg] (left) and [5 mg/Kg] (right). The experimental values of unmetabolized parent compound (dots in the figure) were fitted using Hill type function (line) to obtain a continuous time course of plasma concentration of parent compound; c) metabolite-corrected arterial plasma TACs after intravenous administration of $^{11}$C-labelled AHK2 at [1 µg/Kg] (left) and [5 mg/Kg] (right).

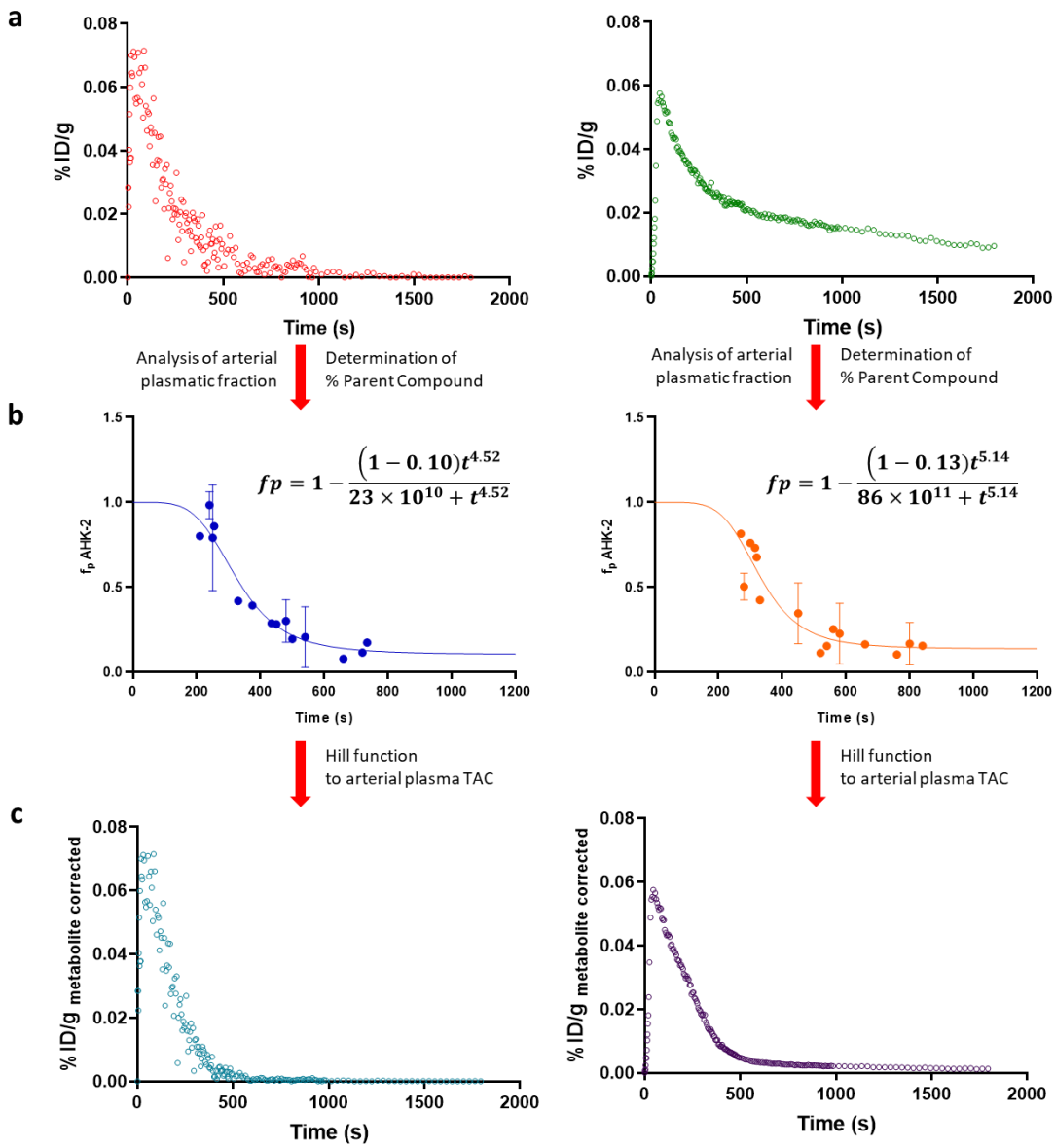


**Figure S7.** Biodistribution of [$^{11}$C]AHK2.1 (a) and [$^{11}$C]AHK2.2 (b) after oral administration (dose = 1 µg/Kg). Representative whole body coronal PET images (projections) obtained at different time points after administration. PET images have been co-registered with a representative CT slice for the anatomical localization of the radioactive signal. Scale bar in in Standard Uptake Value (SUV) units.

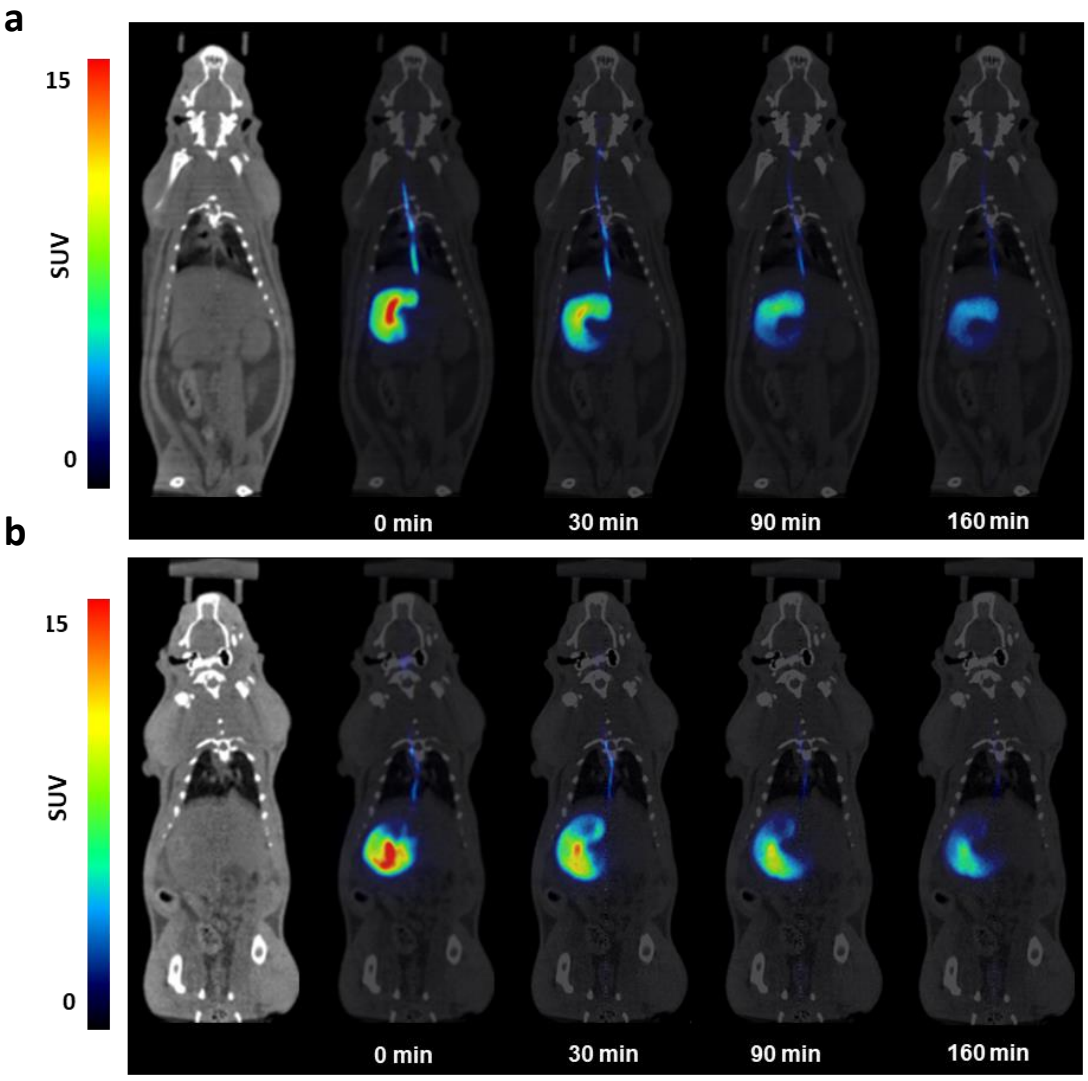


**Figure S8.** $^{1}$H-NMR (400 MHz, $CD_3OD$) and $^{13}$C-NMR (101 MHz, $CD_3OD$) spectra of compound AHK2 (HCl salt).

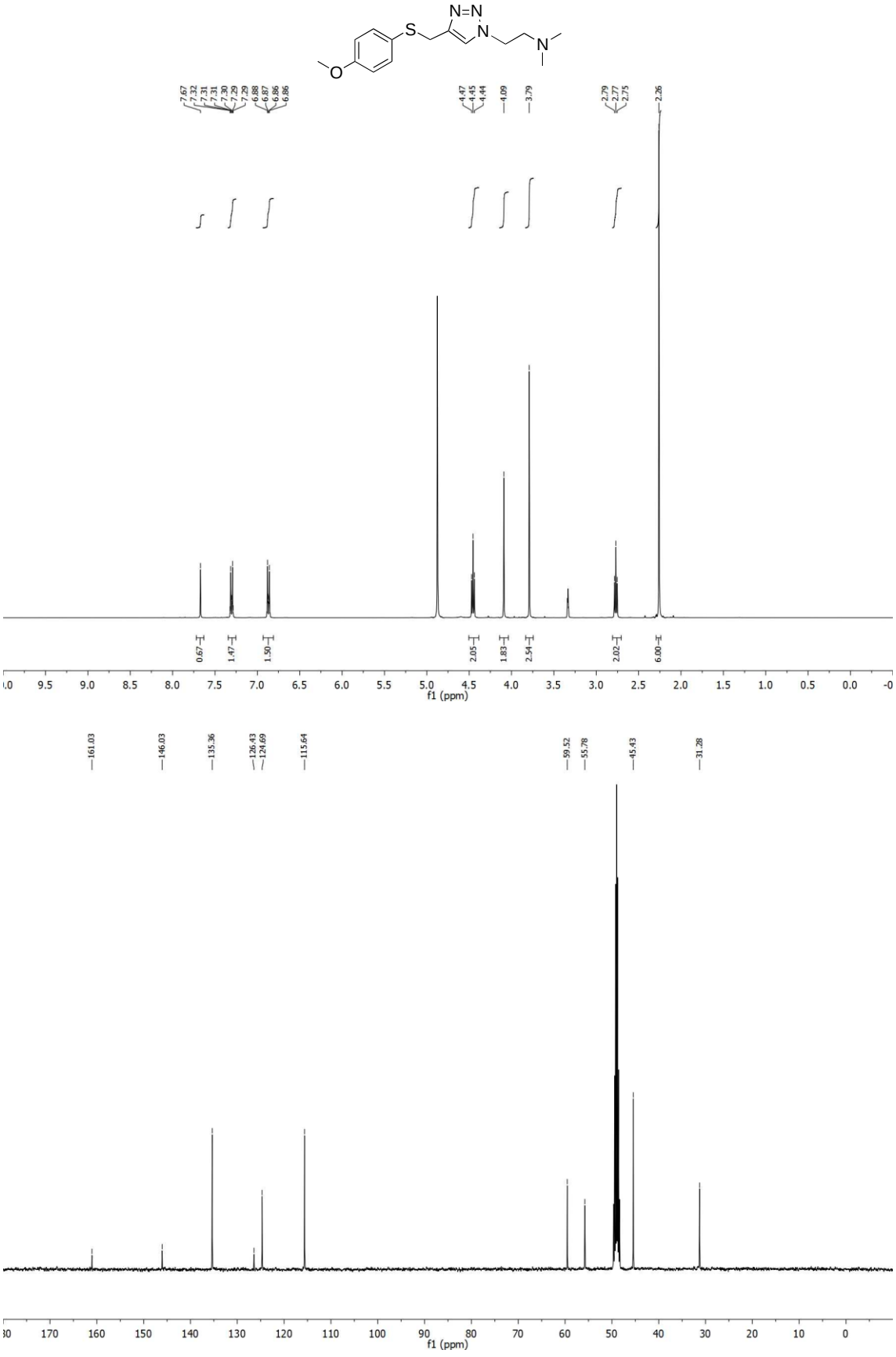


**Figure S9.** $^{1}$H-NMR (400 MHz, $CD_3OD$) and $^{13}$C-NMR (101 MHz, $CD_3OD$) spectra of Precursor **1** (HCl salt).

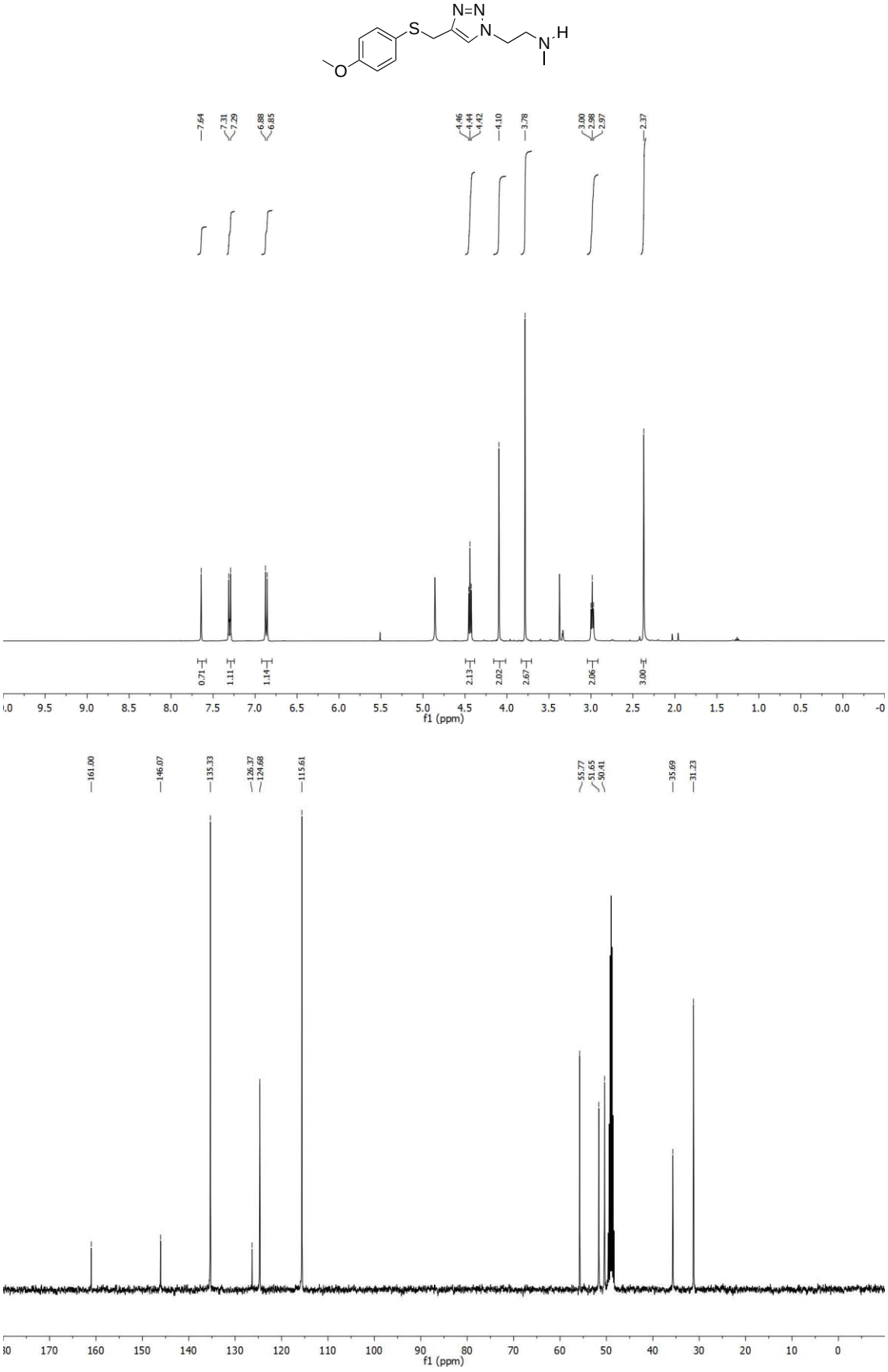


**Figure S10.** $^{1}$H-NMR (400 MHz, $CD_3OD$, HCl salt) and $^{13}$C-NMR (101 MHz, $CDCl_3$) spectra of Precursor **2**.

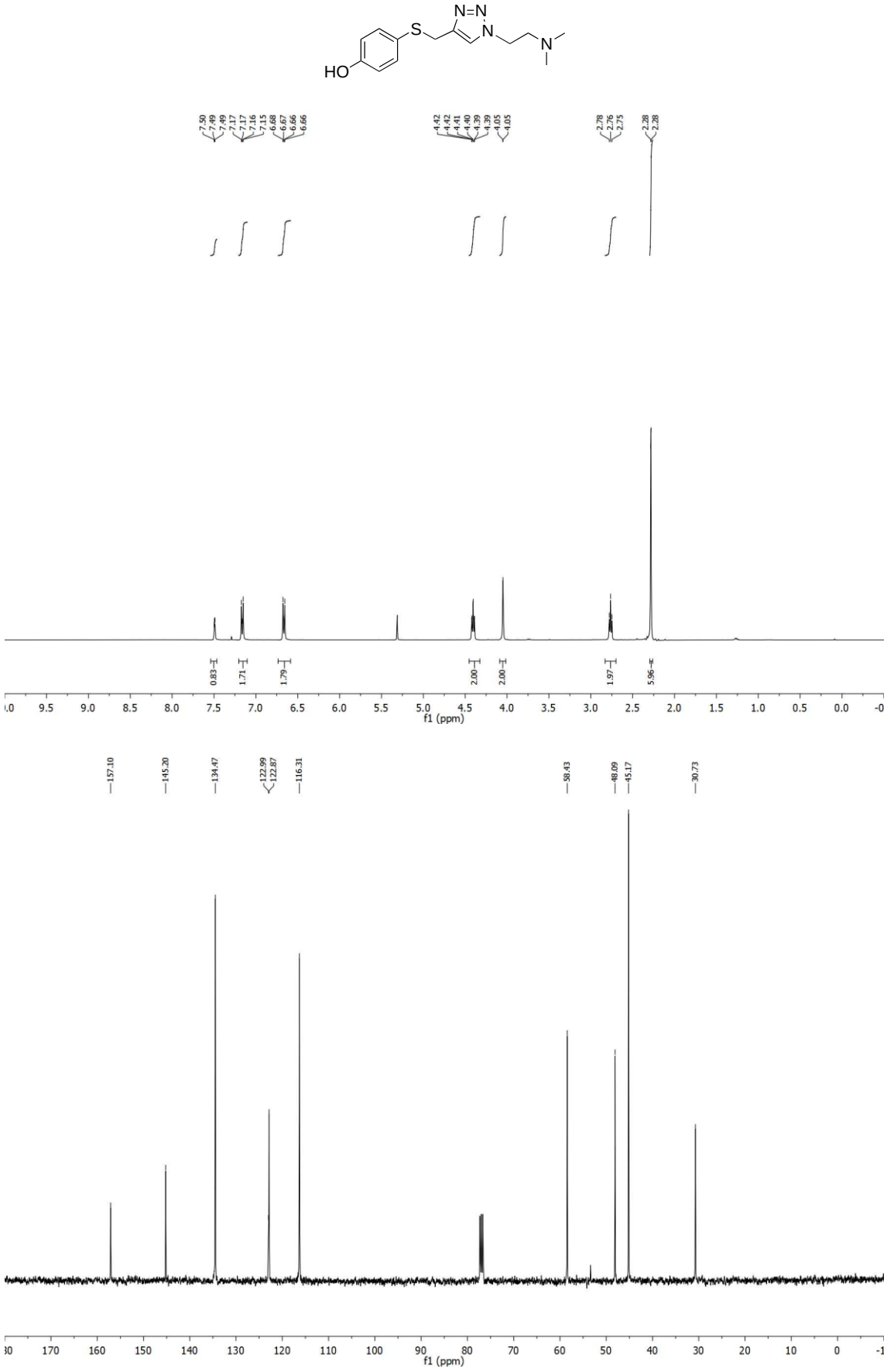
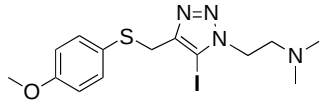
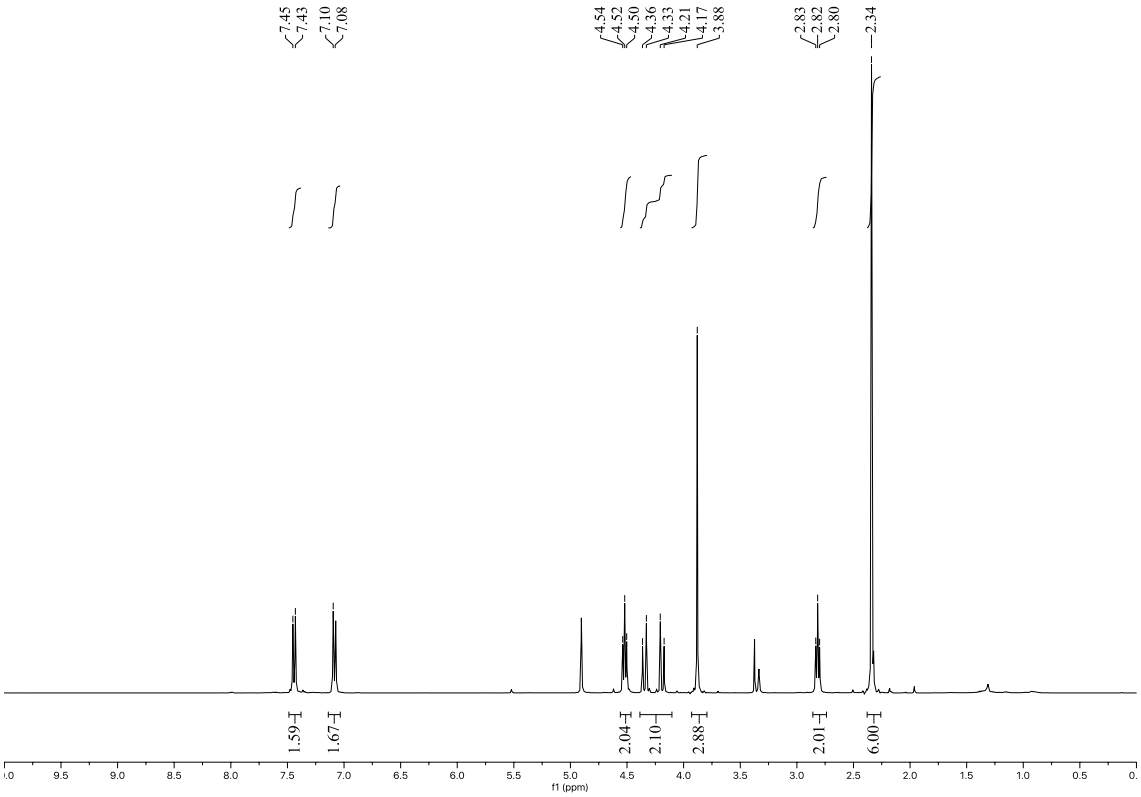


**Figure S11.** $^{1}$H-NMR (400 MHz, $CD_3OD$) and $^{13}$C-NMR (101 MHz, $CD_3OD$) spectra of Precursor **3** (HCl salt).



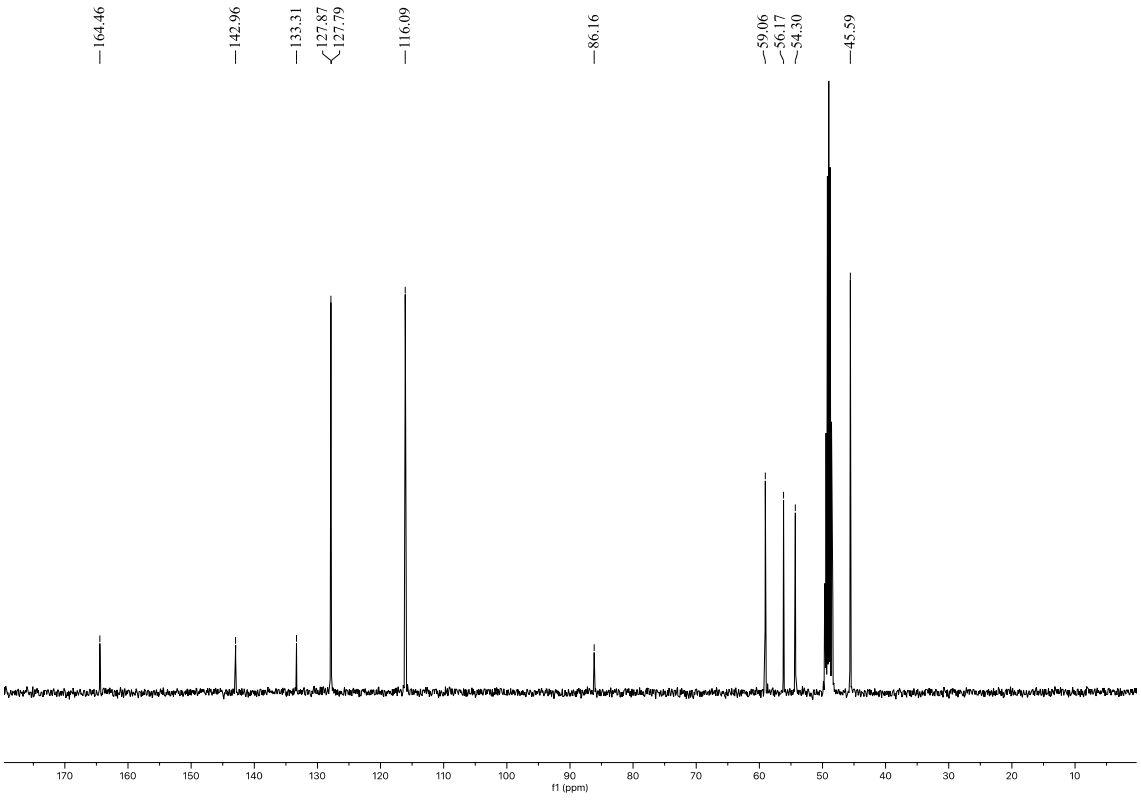



**Figure S12.** HPLC peaks and HR-MS spectra selected for m/z: 309.1 $[M+H]^+$, corresponding to mono-oxidized metabolites of AHK2 obtained in the in vitro metabolism assay. Sulfoxide Met 5 and an isobaric N-oxide are unambiguously detected.

